**Title**
THE USE OF A BORON ADDITION TO PREVENT INTERGRANULAR EMBRITTLEMENT IN Fe-12Mn



**Author**
Hwang, S.K.

**Publication Date**
1979-08-01

# Lawrence Berkeley Laboratory
UNIVERSITY OF CALIFORNIA

## Materials & Molecular Research Division

Submitted to Metallurgical Transactions

THE USE OF A BORON ADDITION TO PREVENT INTERGRANULAR EMBRITTLEMENT IN Fe-12Mn

S. K. Hwang and J. W. Morris, Jr.



August 1979



Prepared for the U.S. Department of Energy under Contract W-7405-ENG-48

## DISCLAIMER

# THE USE OF A BORON ADDITION TO PREVENT INTERGRANULAR EMBRITTLEMENT IN Fe-12Mn

By

S. K. Hwang and J. W. Morris, Jr.

Department of Materials Science and Mineral Engineering and Materials and Molecular Research Division, Lawrence Berkeley Laboratory, University of California, Berkeley, CA. 94720.

## Abstract

Fe-12Mn alloys undergo failure by catastrophic intergranular fracture when tested at low temperature in the as-austenitized condition, a consideration which prevents their use for structural applications at cryogenic temperatures. The present research was undertaken to identify modifications in alloy composition or heat treatment which would suppress this embrittlement. Chemical and microstructural analyses were made on the prior austenite grain boundaries within the alloy in its embrittled state. These studies failed to reveal a chemical or microstructural source for the brittleness, suggesting that intergranular brittleness is inherent to the alloy in the as-austenitized condition. The addition of 0.002 to 0.01 weight percent boron successfully prevented intergranular fracture, leading to a spectacular improvement in the low temperature impact toughness of the alloy. Autoradiographic studies suggest that boron segregates to the austenite grain boundaries during annealing at temperatures near 1000°C. The cryogenic toughness of a Fe-12Mn-0.002B alloy could be further improved by suitable tempering treatments. However, the alloy embrittled if inappropriate tempering

temperatures were used. This temper embrittlement was concomitant with the dissolution of boron from the prior austenite grain boundaries, which re-establishes the intergranular fracture mode.

## INTRODUCTION

The ferritic steels which are currently available for structural use at cryogenic temperatures contain significant nickel alloy additions (5-9 wt.%), with the result that they are relatively expensive. The most obvious element to substitute for nickel in high-alloy steels is manganese, which resembles nickel in many of its chemical and microstructural effects. Research on the cryogenic properties of Fe-Mn alloys has hence been undertaken in a number of laboratories.[1] While prior research has yielded several alloys which retain excellent toughness at cryogenic temperature[2-6], these alloys are austenitic grades which are relatively low in structural strength and very high in manganese content (18-25 wt.%). The development of a ferritic Fe-Mn cryogenic steel poses a recalcitrant problem[7-10] which has been the subject of a continuing research effort in this laboratory.[11-15]

The previous research in this laboratory focused largely on alloys of composition near Fe-12Mn, This composition develops excellent structural strength on cooling to liquid nitrogen temperature (-196°C) but has a relatively high ductile-to-brittle transition temperature due to the onset of intergranular fracture at temperatures only slightly below ambient. The research hence concentrated on the suppression of intergranular fracture. In earlier work[11-14] thermo-mechanical treatments were identified which eliminate intergranular brittleness and impart an excellent strength-toughness combination at -196°C. The treatments required are, however, more elaborate than is desirable in the processing of plate steels. Further research[15] led to the demonstration that intergranular fracture can be suppressed by controlling the rate at which Fe-12Mn is cooled through

the martensite transformation after a normalizing treatment. However, follow-on work revealed that the decrease in the ductile-brittle transition temperature obtained in this way is sensitive to variations in alloy chemistry and heat treatment, with the result that reproducible properties are difficult to obtain. Given the tantalizing, but partial, success obtained it was decided to return to fundamental research into the sources of embrittlement in Fe-12Mn in the hope of identifying a direct and reproducible means for controlling it.

## EXPERIMENTAL PROCEDURE

The alloys described in the following were cast as 10 kg ingots after vacuum induction melting in a helium gas atmosphere. The nominal composition of the base alloy was Fe-12Mn (compositions are given in weight percent unless otherwise noted). Small amounts of titanium (0.1%) and aluminum (0.05%) were added to the base composition to getter interstitial impurities. The boron modified ingots had boron contents from 0.002 to 0.1 weight percent. An analysis of the composition of a nominally Fe-12Mn-0.1Ti-0.05Al-0.002B alloy by optical emission spectroscopy gave the composition: 11.8% manganese, 0.0023% boron, 0.15% Ti, 0.007% Al, 0.007% C, 0.008% N, 0.0024% O, 0.005% P, and 0.006% Si.

The cast ingots were homogenized at 1200°C for 24 hours in an argon atmosphere, were forged, and were then rolled into plates of 13mm thickness. Specimens for mechanical testing were premachined from these plates. Before final machining, all specimens were given an austenitizing treatment at 1000°C for 40 minutes and were then cooled in air. The tempering treatments referred to in the text were conducted on the austenitized blanks and were followed by water quenching.

Charpy impact tests were conducted on 1 cm x 1 cm x 5.5 cm

longitudinal specimens, V-notched according to ASTM specifications. Tensile tests were conducted on sub-sized cylindrical specimens having 13mm gage length and 3mm gage diameter. The tensile specimens were cut with axis parallel to the rolling direction of the plate.

The specimens used for x-ray diffraction analysis, light microscopy, and transmission and scanning electron microscopy were prepared from broken Charpy bars. All x-ray diffraction measurements were made on sections longitudinal to the rolling direction. Auger electron spectroscopic studies were carried out in an Auger electron spectrometer equipped with a fracture stage to prepare surfaces by fracture in vacuum.

An autoradiographic technique[16] was used to monitor the distribution of boron in boron-containing alloys. Metallographically mounted and polished specimens were covered with celluose acetobutyrate replicating tape. They were then exposed to a thermal neutron flux of $4.0 \times 10^9$ $N/cm^2$-sec for three hours. Alpha particles produced by boron isotope decomposition during the irradiation make impact traces on the plastic film. After irradiation the films were removed from the specimens and etched with 10M KOH at 50°C. An incident beam dark field technique in a light microscope was used to record the images of the alpha tracks.

## RESULTS

### a) Sources of Intergranular Failure in Fe-12Mn

The nominally Fe-12Mn alloy becomes brittle at a temperature slightly below room temperature due to the onset of a catastrophic intergranular fracture, as revealed by the scanning electron fractograph presented in Fig. 1. The fracture path follows prior austenite grain boundaries. As discussed in ref. 11 the onset of intergranular fracture is only slightly affected by changes in the austenizing temperature, by normal

variations in the cooling rate, or by minor additions of third alloying elements such as titanium, aluminum, or molybdenum.

Catastrophic intergranular failure in structural steels is usually attributed to one of two causes: the segregation of an embrittling metalloid impurity to the grain boundary, or the development of a second phase along the grain boundary. Both possibilities were investigated.

The segregation of species to the prior austenite grain boundar was monitored through Auger electron spectroscopic analysis of the intergranular fracture surfaces of specimens broken in vacuum. The results have been previously reported[15] and revealed no evidence of significant segregation of a third species. An example Auger spectrum is shown in Fig. 2. A comparison of the Auger spectrum obtained after intergranular fracture with the spectra obtained from fracture surfaces which pass through the bulk of the alloy shows that there are no significant extraneous peaks in the grain boundary pattern. In particular, no significant metalloid peaks were found. The observation that the ductile-brittle transition temperature of the alloy is relatively insensitive to changes in austenitizing time and temperature and to changes in cooling rate (from severe quenching to air cooling) constitutes further evidence that metalloid impurity segregation is not responsible for the intergranular embrittlement of the alloy.

A second possible source of intergranular embrittlement is the intrusion of second phases along the prior austenite grain boundaries. There is, in fact, a logical suspect phase in Fe-12Mn; the hexagonal $\varepsilon$-martensite phase, While Fe-12Mn is predominantly BCC $\alpha'$-martensite in the as-cooled condition, it contains a significant admixture (approximately 15 volume %) of the hexagonal $\varepsilon$-martensite phase. It seems clear

that this hexagonal martensite phase participates in some way in the preference for intergranular failure, since intergranular failure is not normally observed in alloys of lower manganese content, for example, Fe-8Mn[14] in which no ε-martensite is present. Transmission electron microscopic studies were therefore made in a search for ε-martensite in the prior austenite grain boundaries.

The microstructure of a region surrounding a triple point in the prior austenite grain boundary structure is shown in Fig. 3. The major phase present in the microstructures is α'-martensite, which in the case of Fe-12Mn has a somewhat blocky structure. However, no signficant microscopic irregularities were observed at the intersections of the blocky laths of martensite with grain boundaries near the triple point, and no apparent second phase was found along the grain boundary. The distribution of the ε-martensite phase in the vicinity of the prior austenite grain boundaries was specifically studied. The set of transmission electron micrographs presented in Fig. 4 maps a region where crystallites of ε-martensite meet the prior austenite grain boundary. Dark field transmission microscopic studies show no tendency for the epsilon to form as a continuous film along the boundary.

While the results of the present investigation are not fully conclusive, and in particular the presence of an extremely fine grain boundary film cannot entirely be ruled out, the results do suggest that the tendency toward intergranular failure in Fe-12Mn is inherent. A bias toward intergranular failure is, in fact, apparent from the substructure of the alloy, illustrated in Figs. 3 and 4. The grain interiors consist of somewhat irregular martensite blocks surrounded by bands of epsilon phase. An irregular substructure of this type would

be expected to have a significant resistance to transgranular cleavage, with the result that the fracture would tend to seek an easier propagation path along the prior austenite grain boundaries.

b) The Choice of Boron

If the preference for intergranular fracture in Fe-12Mn is an inherent bias due to the relative difficulty of transgranular cleavage, as suggested by the results above, then an appropriate approach to toughen the alloy for cryogenic service would be to add a chemical species which segregates to the prior austenite boundaries and increases their relative cohesion. Boron was selected for this purpose on two grounds. First, the results of research on several ferritic alloys[17-20] suggest that boron has a tendency to segregate to prior austenite grain boundaries, yet improves mechanical properties. Second, an indication of a beneficial effect due to the segregation of boron had been erratically observed in earlier research on Fe-12Mn. Although boron had not been added intentionally to the alloys investigated in earlier phases of the present work, a slight boron segregation was often found in Auger electron spectra from grain boundaries in these alloys, and appeared to be particularly pronounced in those alloys having unusually low transition temperatures.

c) Mechanical Properties of Boron-Modified Alloys

The tensile properties of the Fe-12Mn and Fe-12Mn-0.002B alloys are shown in Table 1. When the alloys were compared in the as-austenitized condition, the addition of boron did not sensibly affect either the tensile strength or the ductility of the Fe-12Mn alloy. However, its influence on the ductile-to-brittle transition temperature was remarkable. The results of Charpy impact tests on Fe-12Mn and on the boron-modified alloys are shown in Fig. 5. The addition of 0.002% and 0.01% boron

suppresses the sharp ductile-to-brittle transition temperature to below -150°C, leading to high impact toughness at liquid nitrogen temperature (-196°C) even in the as-austenitized condition. The upper shelf impact energy, above the transition temperature, was also raised substantially.

The source of the improvement in toughness is the suppression of the intergranular fracture mode, as illustrated in Fig. 6. This figure presents a scanning electron fractograph of the fracture surface of a Charpy specimen of Fe-12Mn-0.002B broken at -196°C. Virtually no intergranular fracture was detected. The fracture mode apparent in the scanning fractograph is transgranular. The fracture surface is rough and irregular on a very fine scale, as was expected as a consequence of the irregular, blocky substructure of the alloy.

It should, however, be noted that, while slight additions of boron proved enormously beneficial to the cryogenic mechanical properties of the alloy, an excessive addition resulted in an overall reduction in toughness. Figure 5 also contains Charpy impact data for an Fe-12Mn-0.1B alloy. This alloy has an upper shelf energy almost 50% below that of the Fe-12Mn base alloy.

Autoradiographic treatments were used to monitor the segregation of boron to prior austenite grain boundaries. The alpha track images of Fe-12Mn-B alloys containing 0, 0.002, 0.01, and 0.05% boron are shown in Fig. 7. Although a quantitative analysis was not attempted, the variation in the amount of boron can easily be seen. A clear network of segregated boron is observed in the sample containing 0.002%B. The size of the network, approximately 100 microns, closely reproduces the average size of the prior austenite grains in the sample. An apparent saturation of the boundaries occurred at approximately 0.01% boron. For

higher boron contents the boundary network is no longer distinguishable. At 0.05% boron some coarse inclusions, as well as stringers, were found along the rolling texture in the alloys. This saturation and consequent precipitation in the matrix is presumably responsible for the decrease in toughness in the 0.1B alloy, as shown in Fig. 5.

On the basis of these investigations the Fe-12Mn-0.002B alloy was selected for further optimization studies.

d) The Effect of Tempering on Mechanical Properties

To explore the effect of subsequent tempering on the mechanical properties of the Fe-12Mn-0.002B alloy, a standard tempering treatment consisting of a one-hour holding followed by water quenching was used for a series of tempering temperatures.

The impact toughnesses of the tempered alloys at -196°C were measured and are plotted in Fig. 8. Both toughness enchancement and temper embrittlement were observed as a consequence of the tempering treatments. Tempering at either 550°C or 650°C increased the impact toughness at -196°C by 20-30% over the toughness in the as-cooled condition. However, tempering at either much higher or much lower temperatures led to a deterioration in toughness accompanied by the re-emergence of the intergranular fracture mode. A sample tempered at 450°C showed a faceted intergranular fracture surface similar to that shown in Fig. 1. Heat treatment at 750°C also resulted in an intergranular fracture mode but in this case with a slight fibrous appearance as shown in Fig. 9.

The results of mechanical property tests on the Fe-12Mn-0.002B alloy tempered at 550°C and 650°C are presented in Fig. 10 and in Table 1. Plots of the Charpy impact energy as a function of temperature (Fig. 10) show that the upper shelf energy of the alloy is lowered by the tempering

treatment but that the toughness at liquid nitrogen temperature is increased. The shape of the curve of toughness vs. temperature is also changed. After tempering the impact toughness of the alloy decreases gradually with decreasing temperature in contrast to the relatively sharp ductile-to-brittle transition encountered when the alloy is tested in the as-cooled condition.

Despite their similar toughnesses, the alloys tempered at 550°C and 650°C were significantly different in their cryogenic tensile properties. As shown in Table 1, tempering at 550°C increased the yield strength of the alloy by approximately 20% over that in the as-cooled condition while tempering at 650°C decreased it by nearly 25%. The yield strength was almost unchanged (decreased ≈ 6%) on tempering at an intermediate temperature of 600°C. All tempering treatments led to an increase in the ultimate tensile strength, with the highest increment (9%) obtained after tempering at 550°C.

To facilitate the interpretation of the mechanical property data, the relative quantities of the phases present in the tempered alloys were determined by x-ray diffraction. The samples examined were cut from the undeformed portions of Charpy specimens tested at -196°C, and are hence representative of the phase distribution present after the sample is cooled to liquid nitrogen temperature, but before mechanical deformation. The results are shown in Fig. 11. Three phases are observed to be present: normal cubic martensite ($\alpha'$), hexagonal epsilon martensite ($\varepsilon$), and austenite ($\gamma$). The maximum amount of retained austenite is present in the sample tempered at 550°C. The epsilon martensite content reaches a maximum at a higher tempering temperature, near 650°C.

Typical microstructures of the tempered alloys are shown in Fig. 12. An analysis of these and other microstructures suggests the following interpretation of the tempering behavior. When the alloy is tempered at temperatures of 500°C or higher, the austenite phase nucleates and grows along the boundaries of the alpha martensite laths. This austenite appears to consume the epsilon martensite which previously decorated the lath boundaries. On tempering at 550°C this reverted austenite has sufficient thermal stability to be retained in the microstructure on subsequent cooling to liquid nitrogen temperature. However, when the tempering temperature is raised to 600°C or higher, the reverted austenite, which is now coarser and presumably leaner in solute content, tends to retransform on cooling to generate an extensive amount of fresh ε-martensite. If the tempering temperature is made higher still, the retransformation reaction continues further and $\alpha'$ martensite becomes the predominant product.

## DISCUSSION

### a) The Sources of Intergranular Brittleness

Brittle fracture due to crack propagation along prior austenite grain boundaries is, of course, a familiar phenomenon which has been widely studied. The typically assumed sources of intergranular fracture are the segregation of metalloid or other impurities to the prior austenite grain boundaries, for example S, P, As, Sb, or Sn[21,22], or the formation of a deleterious grain boundary phase, as, for example, by preferential carbide precipitation[23,24]. However, the available evidence suggests that intergranular brittleness in Fe-12Mn does not arise from either of these causes, but is rather due to an inherent bias toward an intergranular fracture mode in the alloy. The source

of this bias seems clear in the light of results presented in the body of this work: the rather irregular substructure of the polyphase martensite formed on cooling Fe-12Mn causes a high resistance to transgranular cleavage fracture[25], so that the intergranular fracture path is the easier, and hence the preferred, brittle failure mode. This interpretation of the intergranular failure also offers a strightforward explanation for the difference between the spectacular intergranular failure of Fe-12Mn and the equally pronounced transgranular cleavage mode found in Fe-8Mn tested below its ductile-to-brittle transition temperature. The Fe-8Mn alloy forms a lath martensite structure on cooling which resembles that of typical Fe-Ni steels of intermediate nickel content. As in the Fe-Ni steels[25], the laths of martensite within the substructure are well aligned, and permit failure by cooperative cleavage through packets of adjacent laths. The intrusion of the ε-martensite phase in Fe-12Mn leads to an effective decomposition of the martensite substructure, and to the creation of an irregular substructure in which the cooperative cleavage of adjacent elements is relatively difficult. As a consequence, the prior austenite grain boundary becomes the preferred fracture path.

The mechanism is illustrated by the Joffe diagram shown in Fig. 13. A simple but nonetheless useful model of ductile-to-brittle transition behavior is obtained if one assumes a yield strength which increases as temperature decreases and two distinct brittle fracture stresses, one for transgranular cleavage ($\sigma_{fc}$) and one for intergranular failure ($\sigma_{fgb}$), which are relatively insensitive to temperature. The ductile-to-brittle transition is then associated with a change in fracture mode from ductile rupture to brittle fracture when the yield strength rises above

the lower of the two critical fracture stresses. If we assume $\sigma_{fc} < \sigma_{fgb}$ for the 8Mn alloy, which is consistent with its observed fracture mode, and further assume that the shift from 8Mn to 12Mn substantially increases $\sigma_{fc}$ without sensibly changing $\sigma_{fgb}$, then we obtain the relationships shown in Fig. 13. In this case the shift from 8Mn to 12Mn will cause a change in the fracture mode from transgranular cleavage to intergranular failure, but the change in fracture mode will be associated with a decrease rather than an increase in the ductile-to-brittle transition temperature. This behavior is, in fact, observed[2]. The ductile-brittle transition temperature of Fe-12Mn lies approximately 40°C below that of Fe-8Mn when both are tested in the as-austenitized condition.

b) The Beneficial Segregation of Boron

In this, as in other studies, boron appears to be an exceptional and beneficial element in that it segregates to prior austenite grain boundaries and improves mechanical properties[17-20]. It is tempting to describe this effect by saying that boron improves the cohesion of the grain boundaries; however, the effect must be subtle. Elementary thermodynamics[26] shows that any element which preferentially segregates to a grain boundary must lower the interfacial tension of the grain boundary. Deleterious grain boundary additives such as sulfur and phosphorous must hence cause a change in the grain boundary tension which is the same in sign as that caused by boron. Their very different influence on intergranular failure must be due to a difference in the balancing of competing effects.

If we take the simplest possible case, in which the alloy is assumed elastic and the intergranular fracture perfectly brittle, then local crack propagation will be governed by the Griffith criterion[27].

The crack propagates when the energy supplied by the release of stored elastic energy exceeds the energy created by the introduction of fresh surface. In the case of intergranular fracture, the surface energy created on fracture is that associated with the creation of two free surfaces and the destruction of an equivalent area of grain boundary interface. Assuming chemical equilibrium, the net change in surface energy per unit area of fresh fracture surface is $\gamma^* = 2\gamma_s - \gamma_{gb}$, where $\gamma_s$ and $\gamma_{gb}$ are the surface tensions of the free surface and the grain boundary interface respectively. A grain boundary surfactant will promote or retard intergranular fracture in this simple model depending on whether it lowers or raises the net change $\gamma^*$. To be effective in surpressing intergranular fracture a surfactant should hence provide a decrement in the grain boundary tension which is greater than twice its corresponding decrement in the tension of a free surface.

While we know of no directly relevant studies on the effect of boron on surface tension in ferritic alloys, Mortimer[28,29] measured the equilibrium surface and grain boundary tensions of 316 stainless steels with different boron contents. Although the measurements are relatively imprecise and show a significant scatter, an increase in the quantity $2\gamma_s - \gamma_{gb}$ is in fact indicated by some of his measurements on specimens with boron additions.

It should, however, be kept in mind that even when the fracture mode is strikingly intergranular there remains a measureable plastic deformation prior to fracture, as indicated by the tensile elongation values given in Table 1 for the Fe-12Mn alloy. It is hence possible that the beneficial effect of boron is to be associated with a promotion of plastic deformation in the vicinity of the grain boundary rather than with its effect on the grain boundary tension per se. Khachaturyan[30] has, moreover,

pointed out that boron should be a very important stress reliever in Fe-base alloys because of its size difference with the matrix iron atom. Boron may hence segregate so as to relieve stress concentrations at points of high constraint along the grain boundaries which would otherwise be favorable sites for the initiation of intergranular fracture.

c) Temper Embrittlement

The data shown in Fig. 8 suggest that boron-modified Fe-12Mn alloys are susceptible to temper embrittlement if the tempering temperature is either too low, below $\approx$ 500°C, or too high, above $\approx$ 700°C. The available evidence suggests that both these embrittling reactions are associated with the loss of boron from prior austenite boundaries, but for rather different reasons. Autoradiographic studies show that on tempering below 500°C the boron disappears from the prior austenite grain boundaries, and appears to deposit on the martensite lath boundaries. Fig. 14, for example, shows an autoradiograph taken from a sample tempered at 450°C. The grain boundary network of boron is now absent (compare Fig. 7). However, a careful examination of the autoradiograph reveals a finer network of boron traces whose morphology closely resembles the substructure of the $\alpha'$ martensite. When the alloy is tempered at 750°C, on the other hand, it has been heated to above the austenite finish temperature ($A_f$) of this alloy, approximately 680°C, hence regenerating the austenite phase. While 750°C is a sufficiently high temperature to regenerate austenite, it does not appear to be high enough to permit the resegregation of boron to the austenite boundaries in a one-hour temper. As a consequence, after quenching the alloy contains prior austenite boundaries which are not decorated by boron, and the intergranular fracture mode is reestablished.

d) The Beneficial Effect of Intercritical Heat Treatments

The Fe-12Mn alloy shows a favorable response to tempering in the intercritical region between approximately 525°C and approximately 680°C. An examination of the results, as shown for example in Fig. 10 and Table 1, suggests that two rather different reactions are involved in this favorable heat treatment response. When the alloy is given an intercritical temper at approximately 550°C, the predominant effect is the introduction of a significant admixture of austenite phase. The impact toughness at liquid nitrogen temperature is improved with a simultaneous increase in yield strength. When the alloy is heated near the upper end of the intercritical range, near 650°C, the dominant change is the introduction of hexagonal ε-martensite. The impact energy in liquid nitrogen increases also after this treatment, but a concomitant and significant decrease in the alloy yield strength is observed. The strength decrease in the alloy appears to be due to a premature yielding through the stress-induced transformation of the epsilon phase. Since a decrease in the alloy yield strength is usually accompanied by a decrease in the ductile-to-brittle transition temperature, the improvement observed on tempering at 650°C may be simply a consequence of the lower strength associated with the presence of the unstable epsilon phase. On the other hand, the improvement in cryogenic impact properties obtained on tempering at 550°C is associated with the introduction of austenite with an increase in yield strength. The property improvement is, in this case, most probably associated with the removal of unstable ε-martensite coupled with beneficial effects of austenite familiar from the metallurgy of Fe-Ni cryogenic steels[25]. These include the role of austenite in gettering deleterious residual impurities, and its effect in refining the microstructure of the alloy.

## CONCLUSIONS

The principal conclusion from the present work is that it is possible to modify ferritic nickel-free alloys of composition near Fe-12Mn so that they have promising strength-toughness combinations at cryogenic temperatures. A small addition of boron to the Fe-12Mn base metal is sufficient for this purpose and imparts a good combination of cryogenic mechanical properties even in the as-austenitized condition.

Several subsidiary conclusions were also reached in the course of establishing this principal result:

1. The intergranular brittleness of Fe-12Mn alloys in the as-austenitized condition is not due to chemical or microstructural changes in the prior austenite grain boundaries but is rather associated with a change in the preferential fracture path to the grain boundary, presumable because the grain interiors are microstructurally refined.

2. The intergranular brittleness of Fe-12Mn alloys can be prevented by the addition of 0,002-0.01% boron. Boron segregates strongly to the prior austenite grain boundaries. The segregation apparently occurs during austenization at temperatures near 1000°C.

3. If the boron-modified Fe-12Mn alloy is tempered at temperatures below approximately 500°C, the alloy is embrittled and the intergranular fracture mode is reestablished. The embrittlement is associated with a loss of boron from the prior austenite grain boundaries and may involve its segregation to martensite lath boundaries,

4. An Fe-12Mn-0.002B alloy shows a beneficial response to tempering in the range 525-680°C. The breadth of this beneficial tempering range is apparently due to the overlap of two rather different mechanisms. On tempering near 550°C an admixture of austenite is retained in the matrix,

and the toughness increases without loss in strength, as is observed in typical Fe-Ni cryogenic steels given similar intercritical tempering treatments. If the alloy is heat treated near 650°C, a large admixture of the epsilon martensite phase results. The cryogenic toughness is improved, but at considerable cost in the yield strength of the alloy.

5. When an Fe-12Mn-0.002B alloy is heat treated at temperatures above 680°C, near 700°C, the alloy is again embrittled. The embrittlement is, in this case, believed to be due to the creation of fresh austenite grain boundaries at a temperature too low for the resegregation of boron in a reasonable tempering time.

## ACKNOWLEDGEMENTS

The authors are grateful to Mr. W. Love for his assistance in the boron autoradiography, and to Professor Gabor Somorjai and several of his students for assistance in Auger analysis. This research was supported by the Division of Materials Sciences, Office of Basic Energy Sciences, U.S. Department of Energy under Contract No. W-7405-Eng-48.

REFERENCES

1. J. W. Morris, Jr., S. K. Hwang, K. A. Yuschenko, V. T. Belotzerkovetz, and O. G. Kvasnevskii: Advances in Cryogenic Engineering, 1978, vol. 24, p. 91.

2. M. J. Schanfein, M, J. Yokata, V. F. Zackay, E. R. Parker, and J. W. Morris, Jr.: Properties of Materials for Liquified Natural Gas Tankage, ASTM STP 579, 1975, p. 361.

3. H. Yoshimora, N. Yamada, and H. Yada: Trans. Iron Steel Inst. Japan, 1976, vol. 15, p. 464.

4. T. Kato, S. Fukui, M. Fujikura, and K. Ishida: Trans. Iron Steel Inst. Japan, 1976, vol. 16 p. 673.

5. K. A. Yushchenko: Advances in Cryogenic Engineering, 1978, vol. 24, p. 120.

6. R. L. Tobler, H. J. McHenry, and R. P. Reed: Advances in Cryogenic Engineering, 1978, vol. 24, p. 560.

7. M. J. Roberts: Met. Trans., 1970, vol. 1, p. 3287.

8. A. Holden, J. D. Bolton, and E. R. Petty: J. Iron Steel Inst., 1971, vol. 209, p. 721.

9. J. D. Bolton, E. R. Petty, and G. B. Allen: Met. Trans., 1971, vol. 2, p. 2915.

10. R. L. Miller: "Manganese", special issue of Materiaux et Techniques, Dec., 1977, p. 55.

11. S. K. Hwang, S. Jin, and J. W. Morris, Jr.: Proc. 4th Int. Conf., Strength of Metals and Alloys, Laboratoire de Physique du Solide, Nancy, France, 1976, vol. 2, p. 842.

12. S. K. Hwang and J. W. Morris, Jr.: Proceedings, USSR-US Seminar on Applied Problems of Low Temperature Materials, E. O. Paton Inst. of

of Electro-welding, Kiev, USSR, 1976.

13. S. K. Hwang, PhD thesis, Dept. Materials Science and Engineering, University of California at Berkeley, Berkeley, CA, 1977.

14. S. K. Hwang and J. W. Morris, Jr.: Met. Trans. (In press).

15. S. K. Hwang and J. W. Morris, Jr.: Advances in Cryogenic Engineering, 1978, vol. 24, p. 137,

16. Y. L. Chen, PhD thesis, Dept. Materials Science and Engineering, University of California at Berkeley, Berkeley, CA, 1976.

17. H. Taga and A. Yoshikawa: Trans. Iron Steel Inst. Japan (Suppl.), 1971, vol. 11, p. 1256.

18. T. M. Williams, D. R. Harris, and J. Furnival: J. Iron Steel Inst., 1972, vol. 210, p. 351.

19. G. F. Melloy, P. R. Slimmon, and P. P. Podgursky: Met. Trans., 1973, vol. 4, p. 2279.

20. M. V. Mozharov, L. L. Pyatakova, and M. A. Sirotkina: Fiz. Metal. Metalloved, 1975, vol. 40, p. 215.

21. A. Joshi and D. F. Stein: Temper Embrittlement of Alloy Steels, ASTM STP, 1972, vol. 499, p. 59.

22. H. L. Marcus, L. H. Hackett, Jr., and P. W. Palmberg: ibid., p. 90.

23. C. J. McMahon, Jr.: Grain Boundaries in Engineering Metals, J. L. Walter, J. H. Westbrook and D. A. Woodford, eds., Claitor's Pub. Co., New Orleans, 1975, p. 525.

24. G. Thomas: Met. Trans., 1978, vol. 9A, p. 439.

25. J. W. Morris, Jr., C. K. Syn, J. I. Kim, and B. Fultz: Proceedings, International Conference on Martensitic Transformation (ICOMAT), Cambridge, Massachusetts, June, 1979 (In press).

26. J. W. Gibbs: Scientific Papers: Vol. I: Thermodynamics, Dover, New York, 1961, p. 240.

27. A. A. Griffith: Phil. Trans. Roy. Soc. (London), 1921, vol. A221, p. 163.

28. D. A. Mortimer: Grain Boundaries in Engineering Metals, J. L. Walter, J. H. Westbrook, and D. A. Woodford, eds., Claitors Pub., New Orleans, 1975, p. 647.

29. D. A. Mortimer and M. G. Nichols: J. Met. Sci., September, 1976, p. 326.

30. A. G. Khatchaturyan: Private Communication.

TABLE 1. Mechanical Properties of Fe-12Mn Alloys.

| Composition and Treatment | Test Temp. (°C) | $\sigma_y$ (MPa) | $\sigma_{uts}$ (MPa) | Uniform Elong. (%) | Total Elong. (%) | Red. in Area (%) |
|---|---|---|---|---|---|---|
| Fe-12Mn-0.2Ti (From Ref. 6) | 25 | 600 | 924 | 6 | 25 | 78 |
| As Austenitized (900°C/2 hrs/WQ) | -196 | 889 | 1351 | 11 | 25 | 54 |
| Fe-12Mn-0.1Ti-0.05Al-0.002B | 25 | 633 | 981 | 7 | 26 | 77 |
| As Austenitized (1000°C/40 min./AC) | -196 | 854 | 1414 | 12 | 26 | 66 |
| 550°C/1 hr/WQ | 25 | 733 | 1043 | 12 | 31 | 79 |
| | -196 | 1036 | 1539 | 19 | 34 | 65 |
| 600°C/1 hr/WQ | 25 | 600 | 1036 | 13 | 28 | 78 |
| | -196 | 807 | 1493 | 19 | 30 | 62 |
| 650°C/1 hr/WQ | 25 | 374 | 1059 | 11 | 29 | 79 |
| | -196 | 649 | 1488 | 16 | 27 | 63 |

FIGURE CAPTIONS

Fig. 1. Fe-12Mn, as-austenitized (1000°C/40 min./air cooled): Scanning electron fractographs of the surface of a Charpy specimen broken at -196°C.

Fig. 2. Fe-12Mn, as-austenitized (1100°C/2 hrs/water quenched): Auger electron spectrum from a surface created through intergranular fracture in vacuum at -145°C, showing grain boundary composition.

Fig. 3. Fe-12Mn, as-austenitized (1000°C/40 min./air cooled): Transmission electron micrograph showing the microstructure of a region surrounding a triple point in the prior austenite grain boundary network.

Fig. 4. Fe-12Mn, as-austenitized (1000°C/40 min/air cooled): Transmission electron micrographs of a region where the epsilon (ε) martensite meets the prior austenite grain boundaries. (a) Bright field (b) Dark field image of ε.

Fig. 5. Fe-12Mn-B alloys, as-austenitized (1000°C/40 min./air cooled): Charpy V-notch impact energy as a function of temperature.

Fig. 6. Fe-12Mn-01Ti-0.05Al-0.002B, as-austenitized (1000°C/40 min./air cooled); Scanning electron fractograph of a Charpy specimen broken at -196°C.

Fig. 7. Fe-12Mn-B alloys, as-austenitized (1000°C/40 min./air cooled): Boron autoradiographs (a) 0% B (b) 0.002% B (c) 0.01% B (d) 0.05% B (e) 0.1% B.

Fig. 8. Fe-12Mn-0.1Ti-0.05Al-0.002B, tempered for one hour and water quenched: Charpy impact toughness (CVN) at -196°C as a function of tempering temperature.

Fig. 9. Fe-12Mn-0.1Ti-0.05Al-0.002B, tempered for one hour at 750°C and water quenched: Scanning electron fractograph of a Charpy specimen broken at -196°C.

Fig. 10. Fe-12Mn-0.1Ti-0.05Al-0.002B. Charpy V-notched impact toughness (CVN) as a function of temperature for different heat treatments.

Fig. 11. Fe-12Mn-0.1Ti-0.05Al-0.002B, tempered for one hour, water quenched, and cooled to -196°C: Volume percent of $\gamma$ and $\varepsilon$ phases as a function of tempering temperatures.

Fig. 12. Fe-12Mn-0.1Ti-0.05Al-0.002B, tempered for one hour and water quenched: Microstructures of the heat treated specimens. (a) 550°C/1 hr. (b) 650°C/1 hr. TEM.

Fig. 13. Hypothetical Joffee diagram relating the yield stress ($\sigma_y$), the fracture stress for transgranular cleavage ($\sigma_{fc}$) and the fracture stress for intergranular crackings ($\sigma_{fgb}$) of Fe-12Mn and Fe-8Mn alloys with respect to temperature.

Fig. 14. Fe-12Mn-0.1Ti-0.05Al-0.002B, retempered at 450°C for one hour, water quenched: Autoradiograph showing the disappearance of boron from grain boundaries. A fine network of boron traces is, however, visible, suggesting that boron re-deposits on martensite lath boundaries.

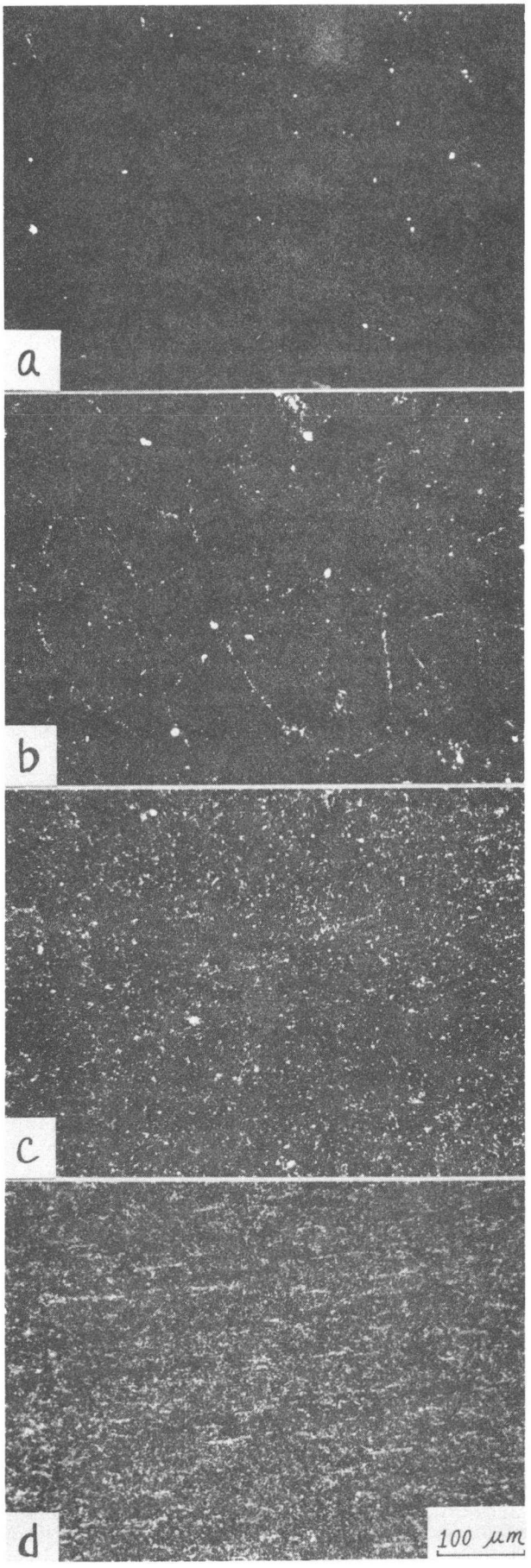


XBB791-0408

Figure 1

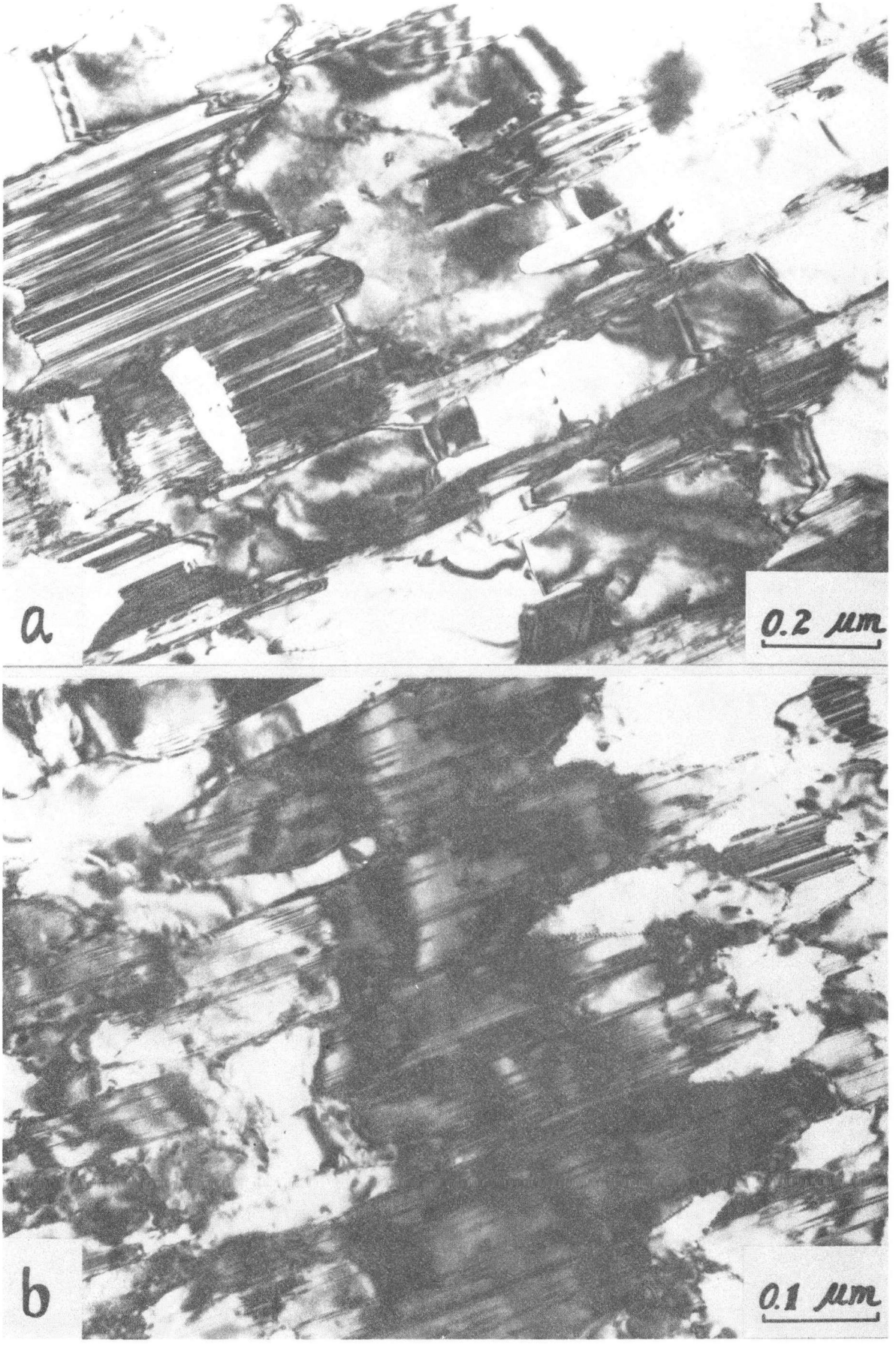


Figure 2

XBB791-0407

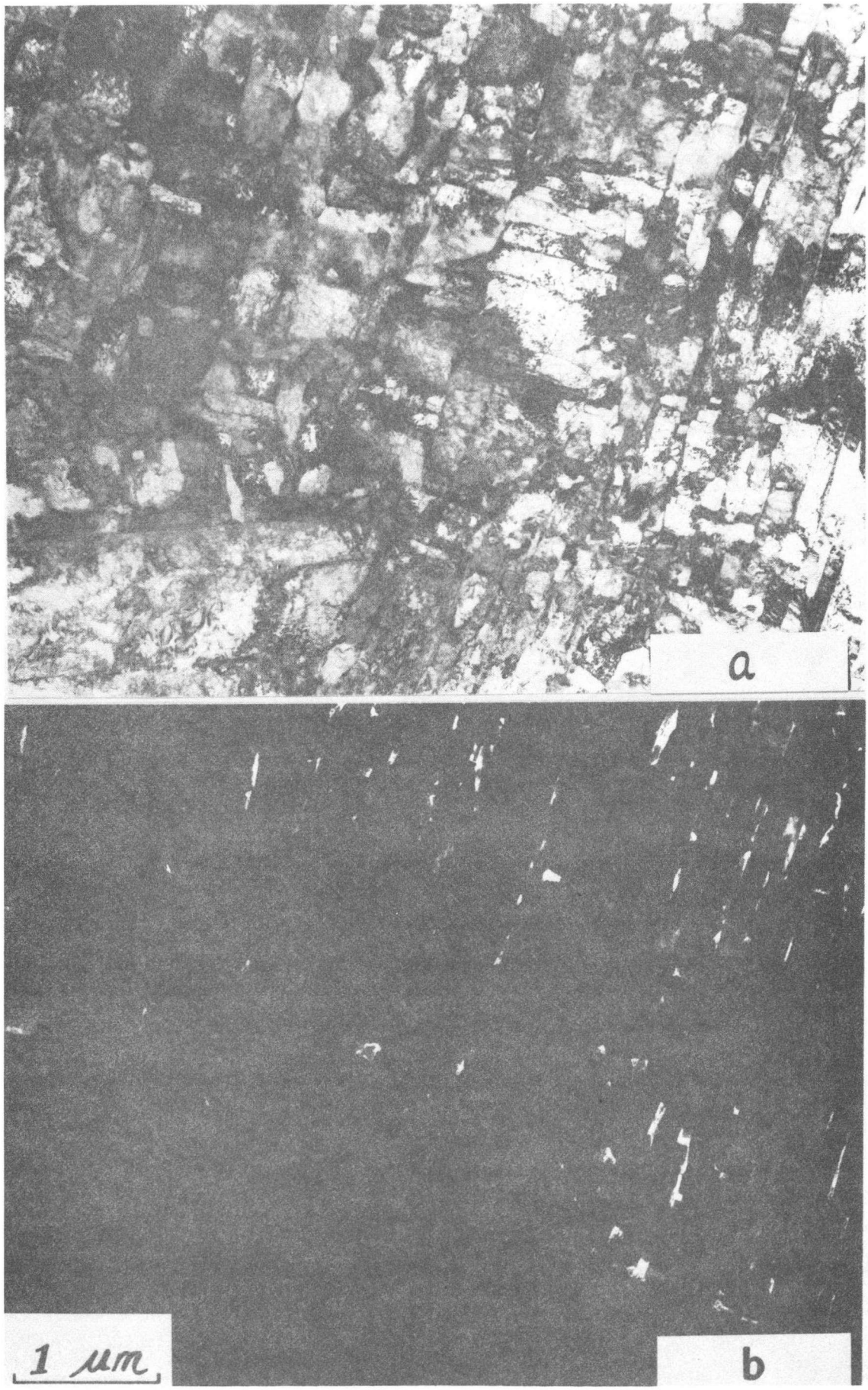


Figure 3

XBB791-0406

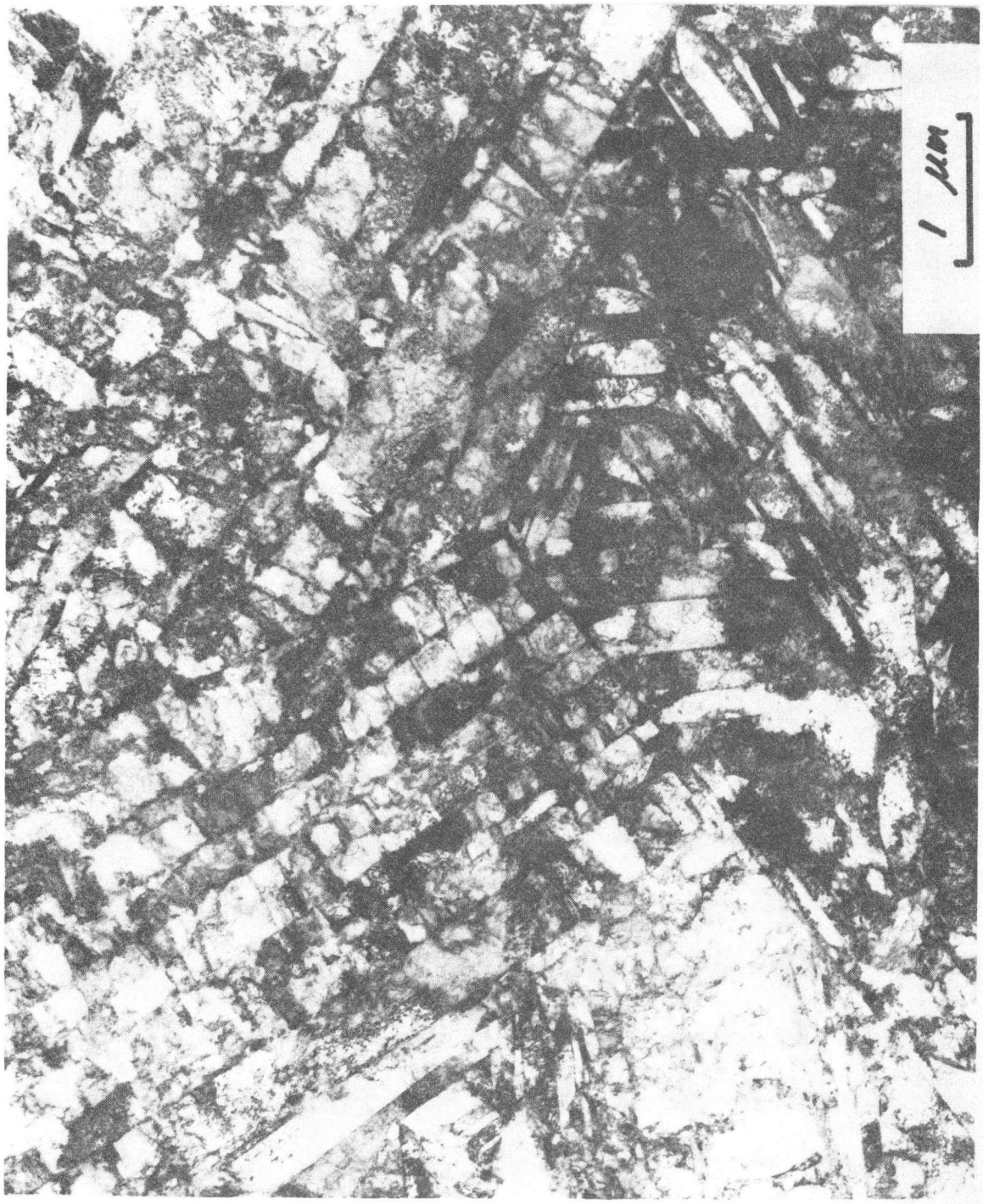


Figure 4

XBB791-0405

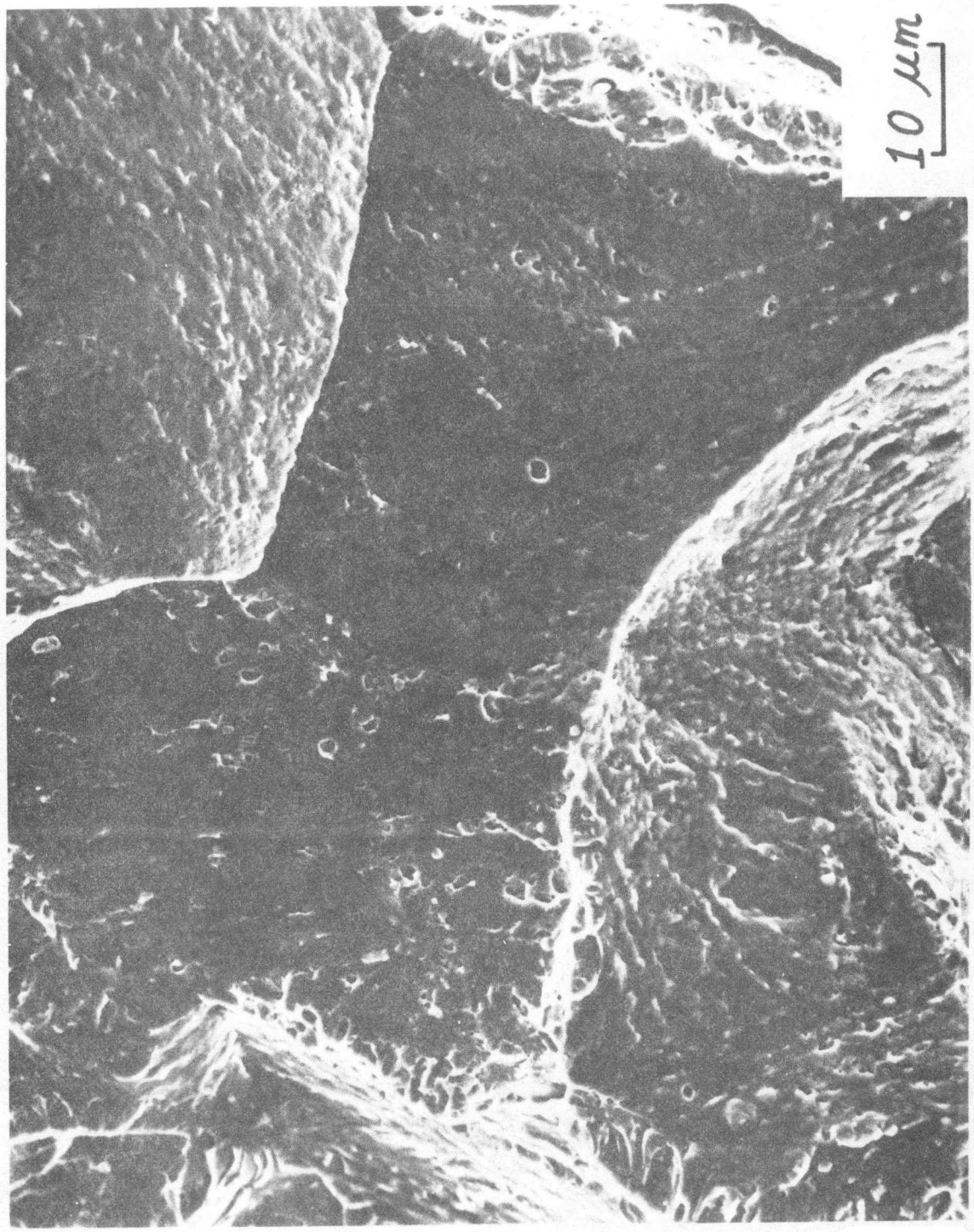


Figure 5

XBB791-0404

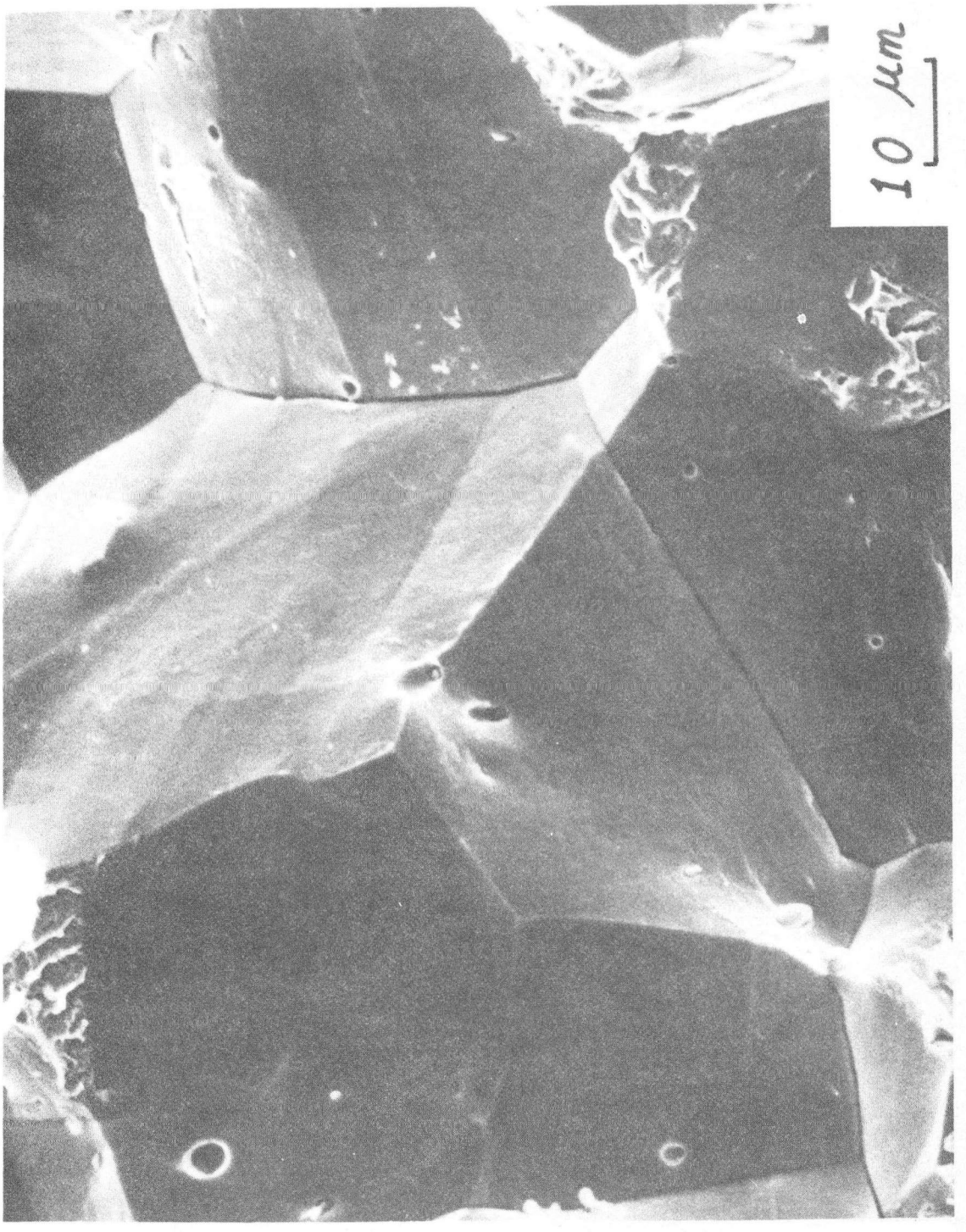


Figure 6

XBB791-0403

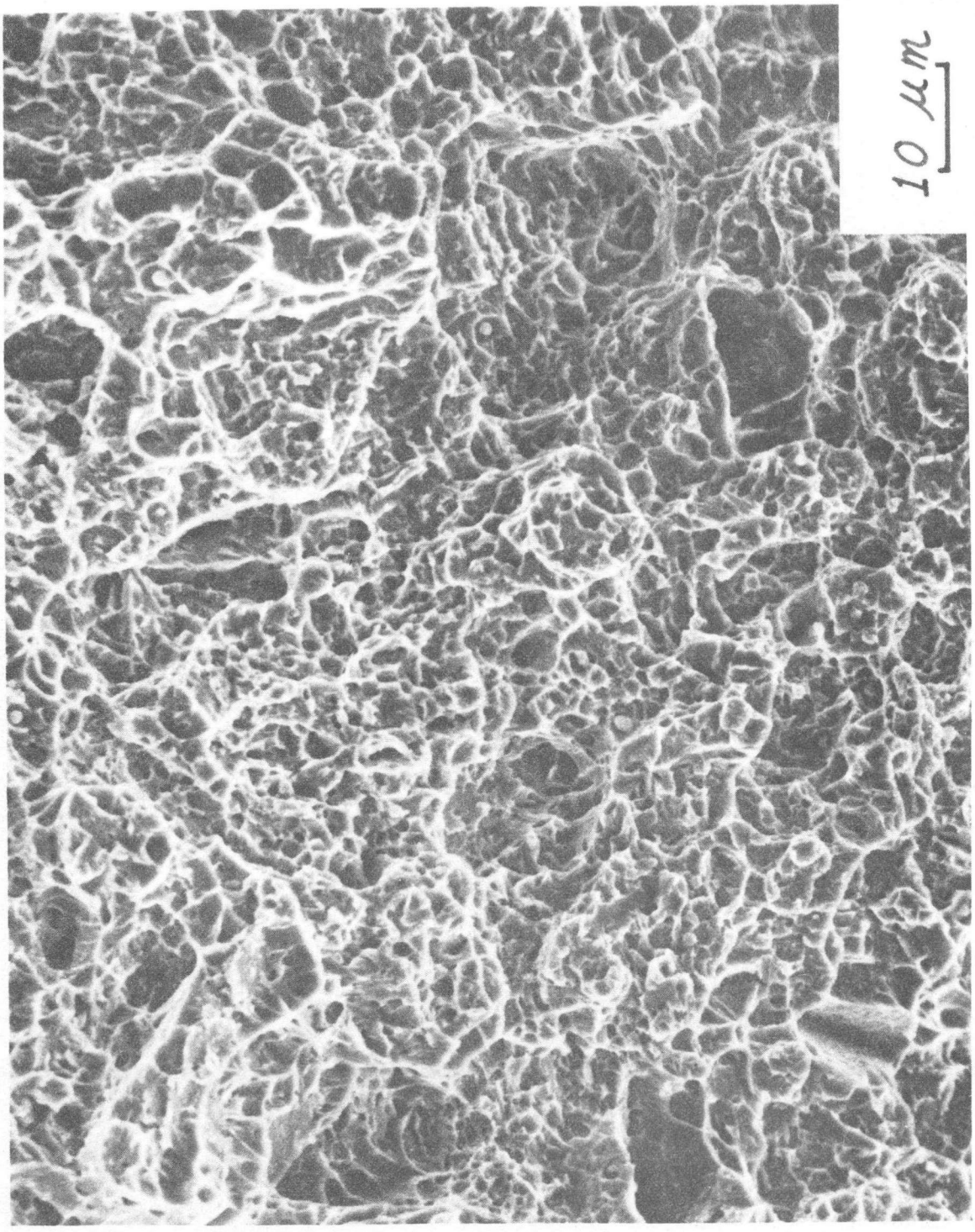


Figure 7

XBB791-0402

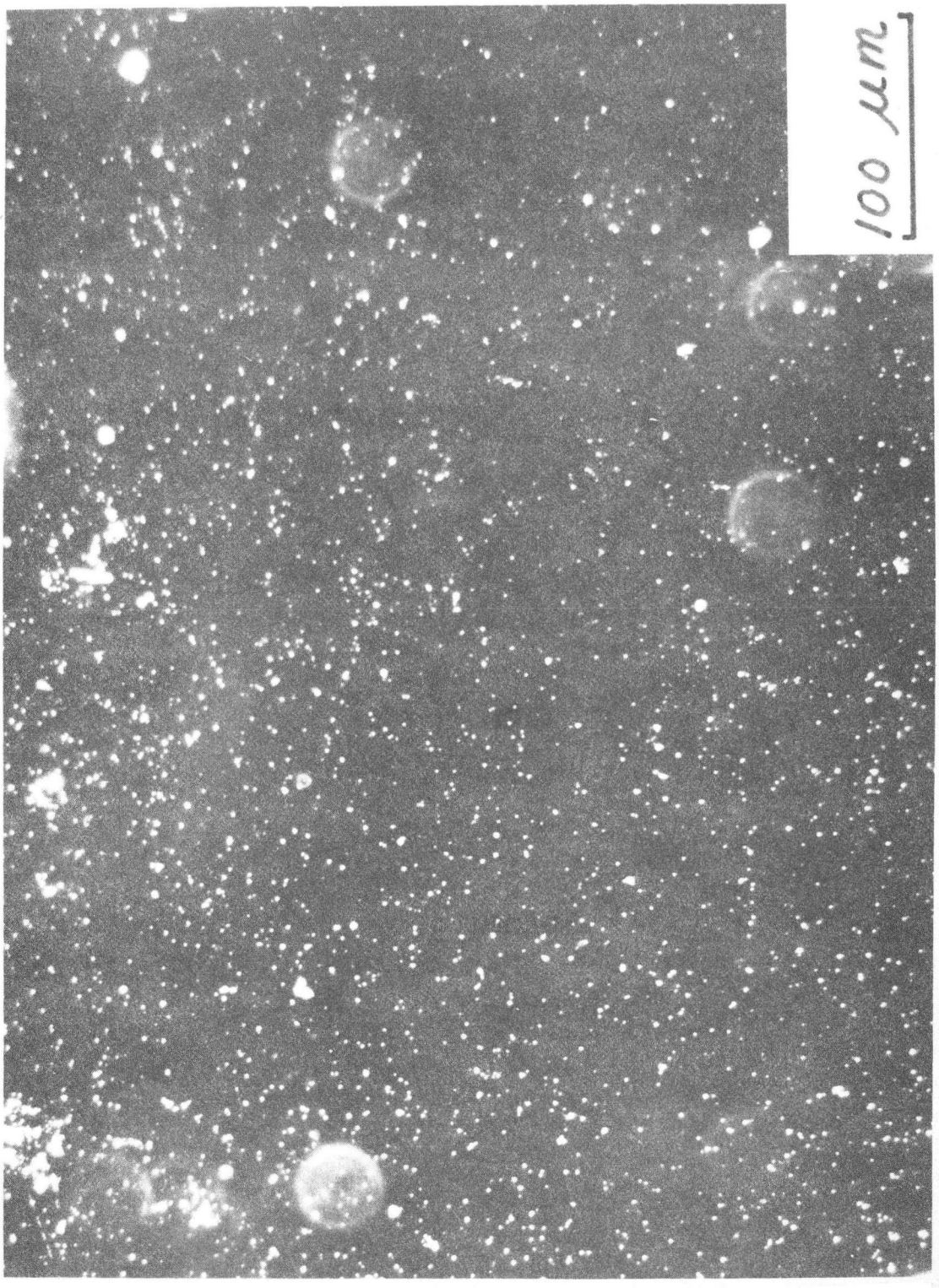


Figure 8

XBB791-0401

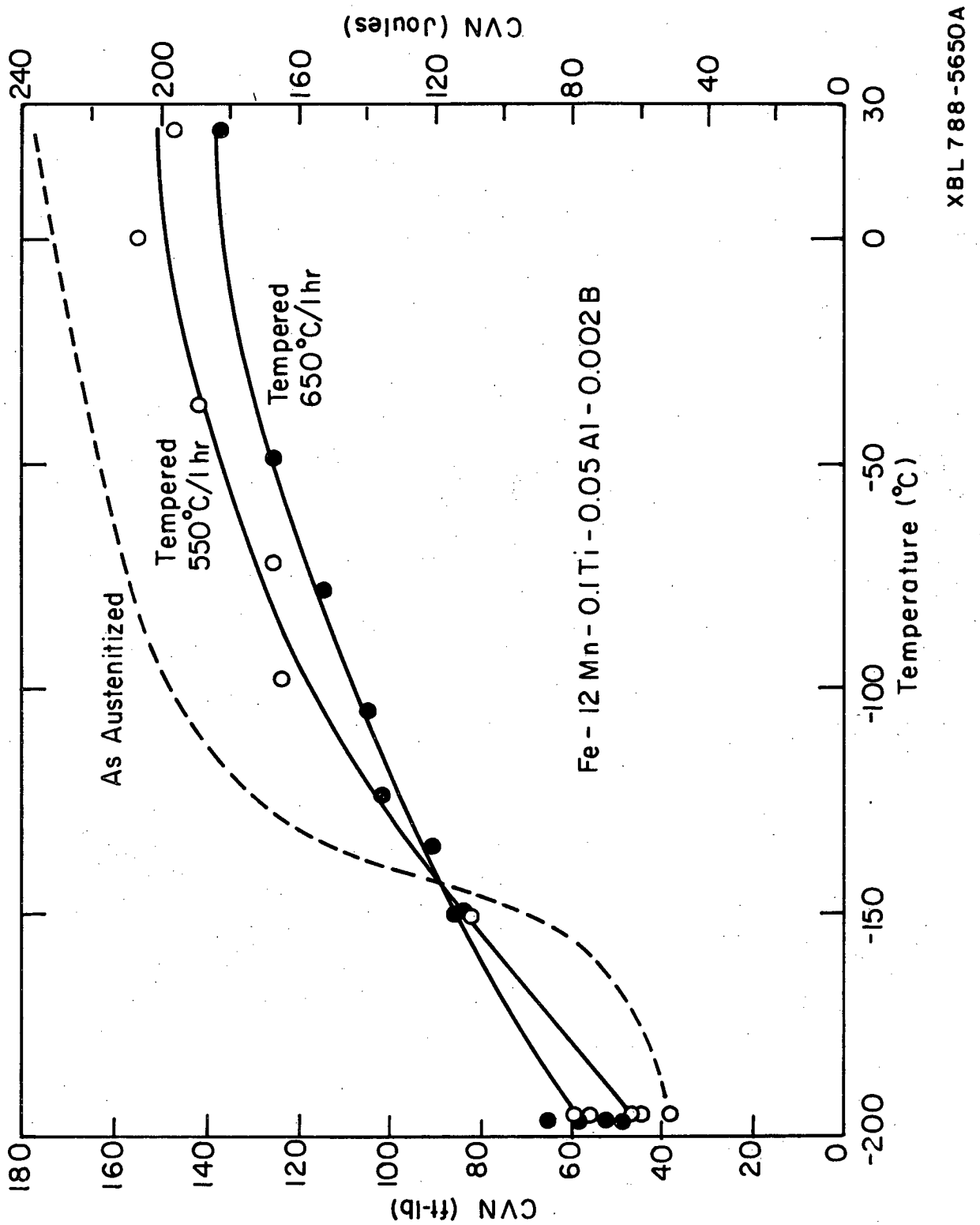
CVN (ft-lb)
CVN (Joules)
Temperature (°C)
Fe - 12 Mn - 0.1 Ti - 0.05 Al - 0.002 B
As Austenitized
Tempered 550°C/1 hr
Tempered 650°C/1 hr
XBL 788-5650A

Figure 9

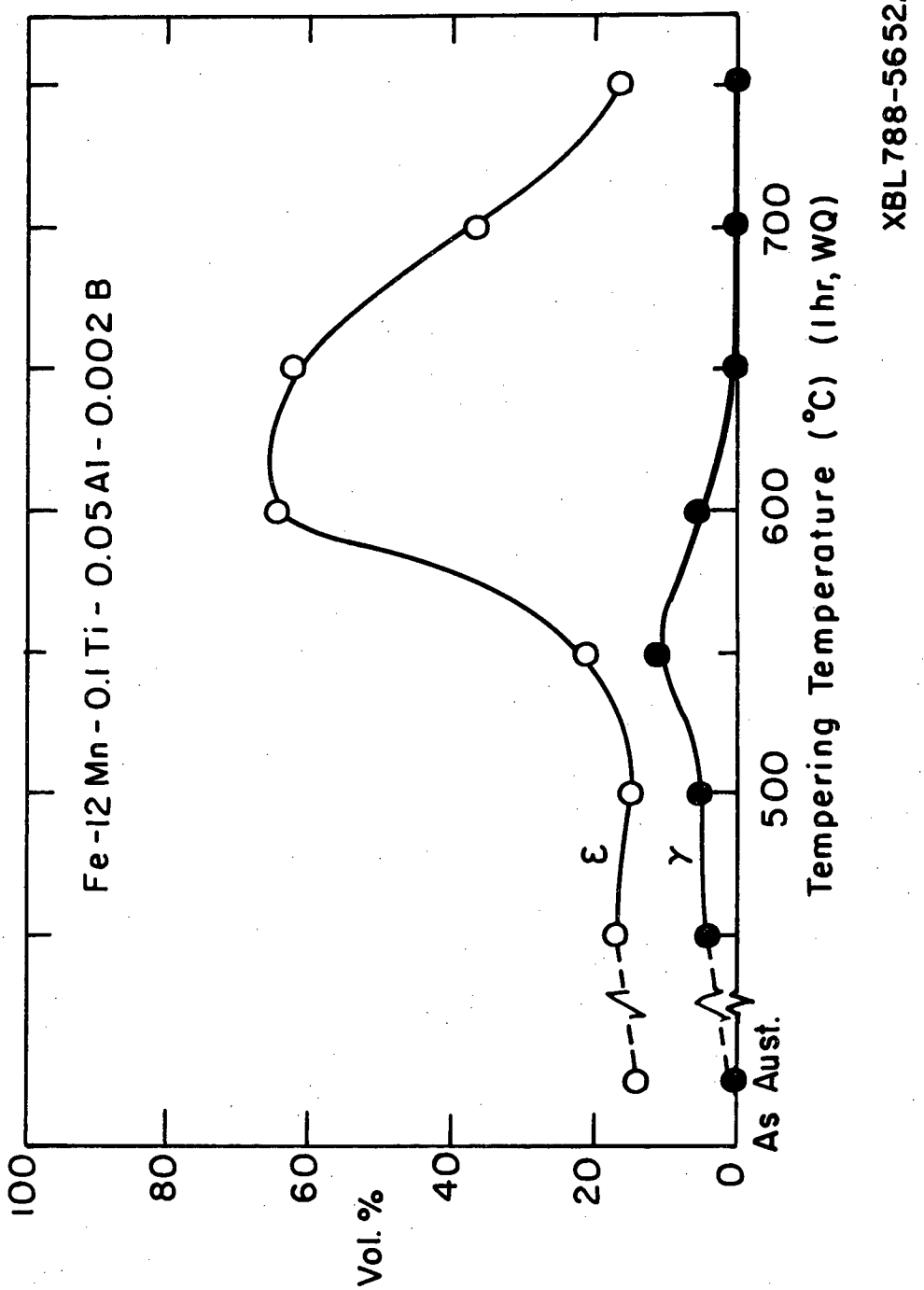


XBL 788-5652A

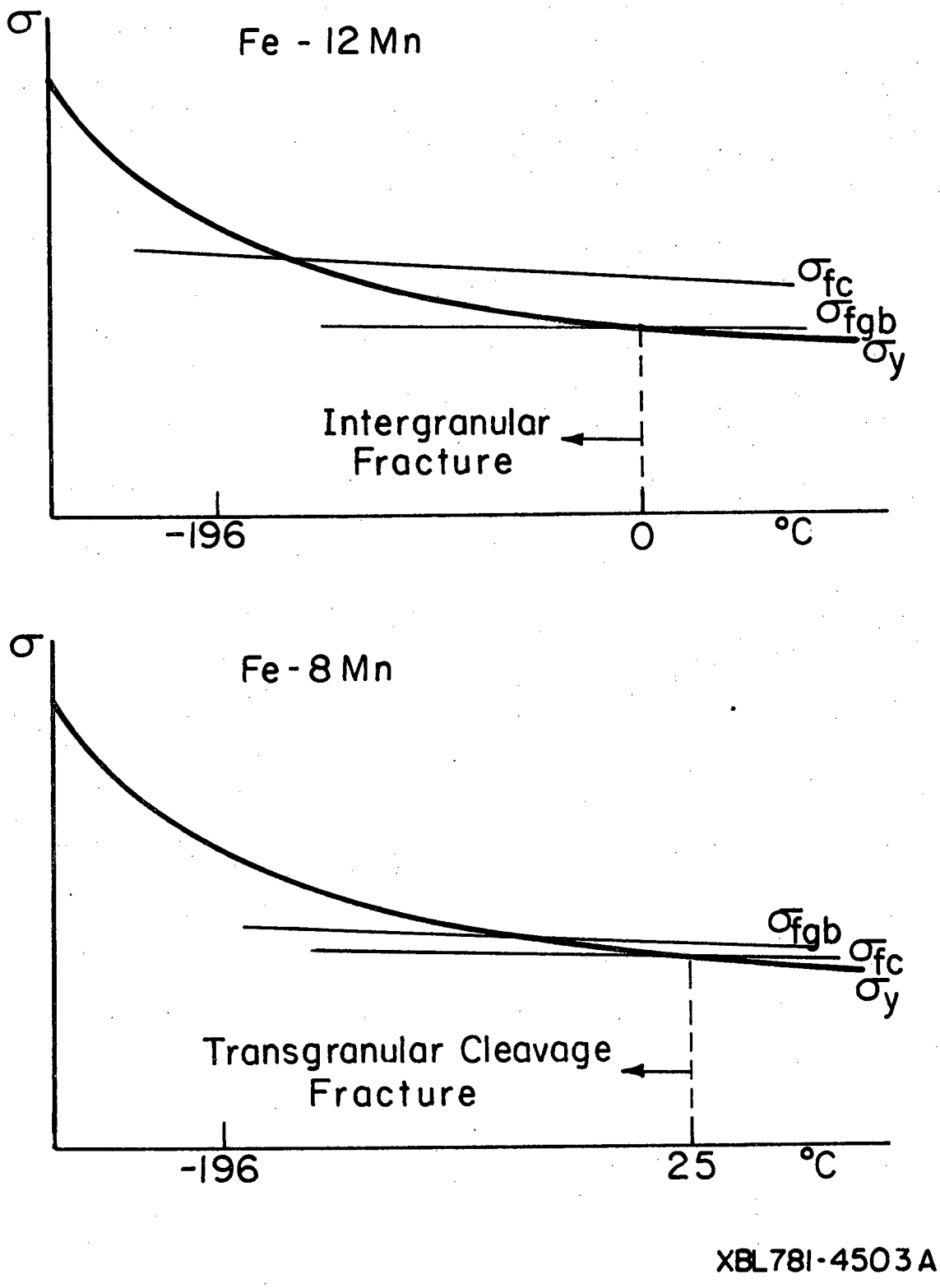
σ
Fe - 12 Mn
σfc
σfgb
σy
Intergranular
Fracture
-196
0
°C
σ
Fe - 8 Mn
σfgb
σfc
σy
Transgranular Cleavage
Fracture
-196
25
°C
XBL781-4503A

Figure 10

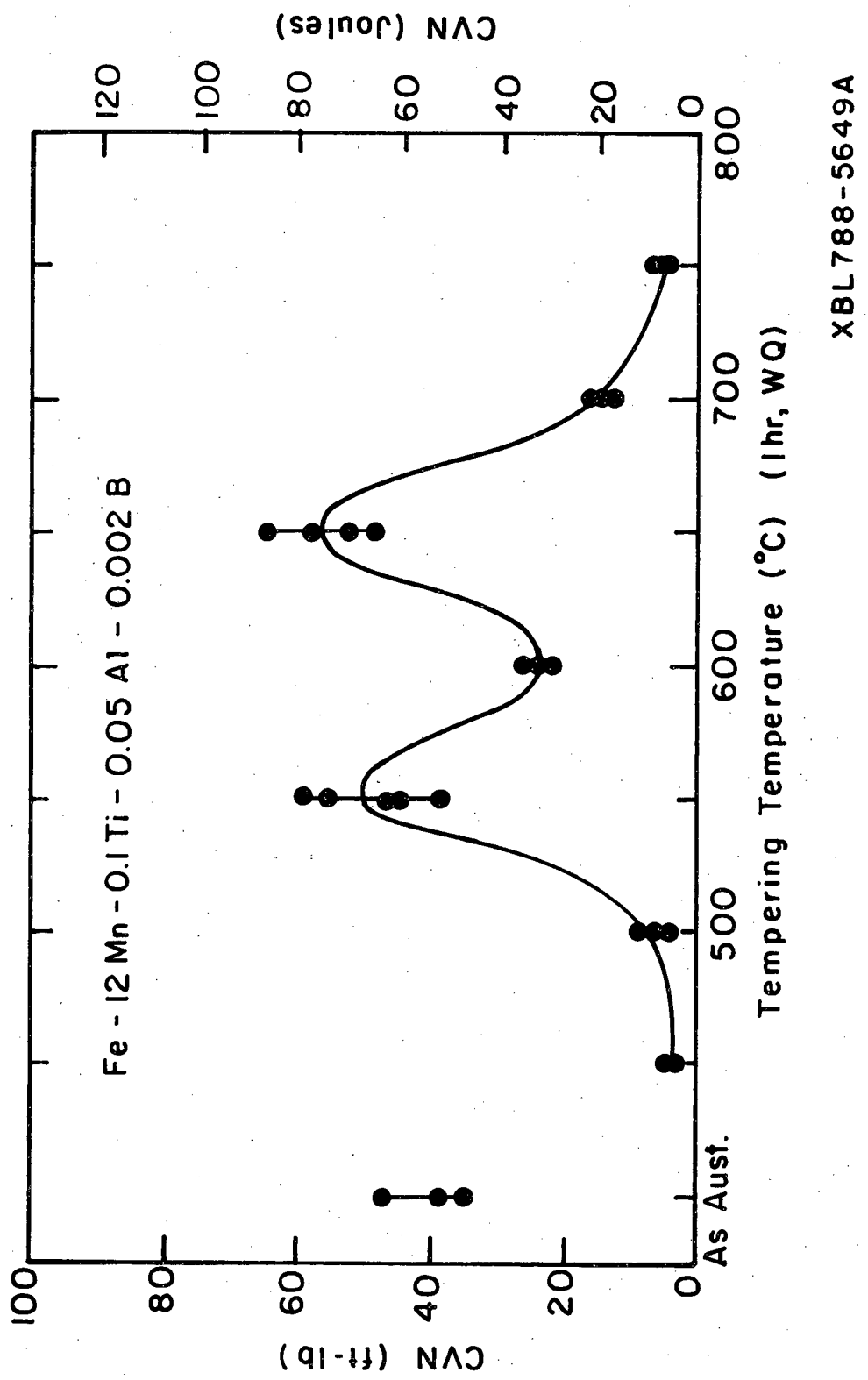


Figure 11

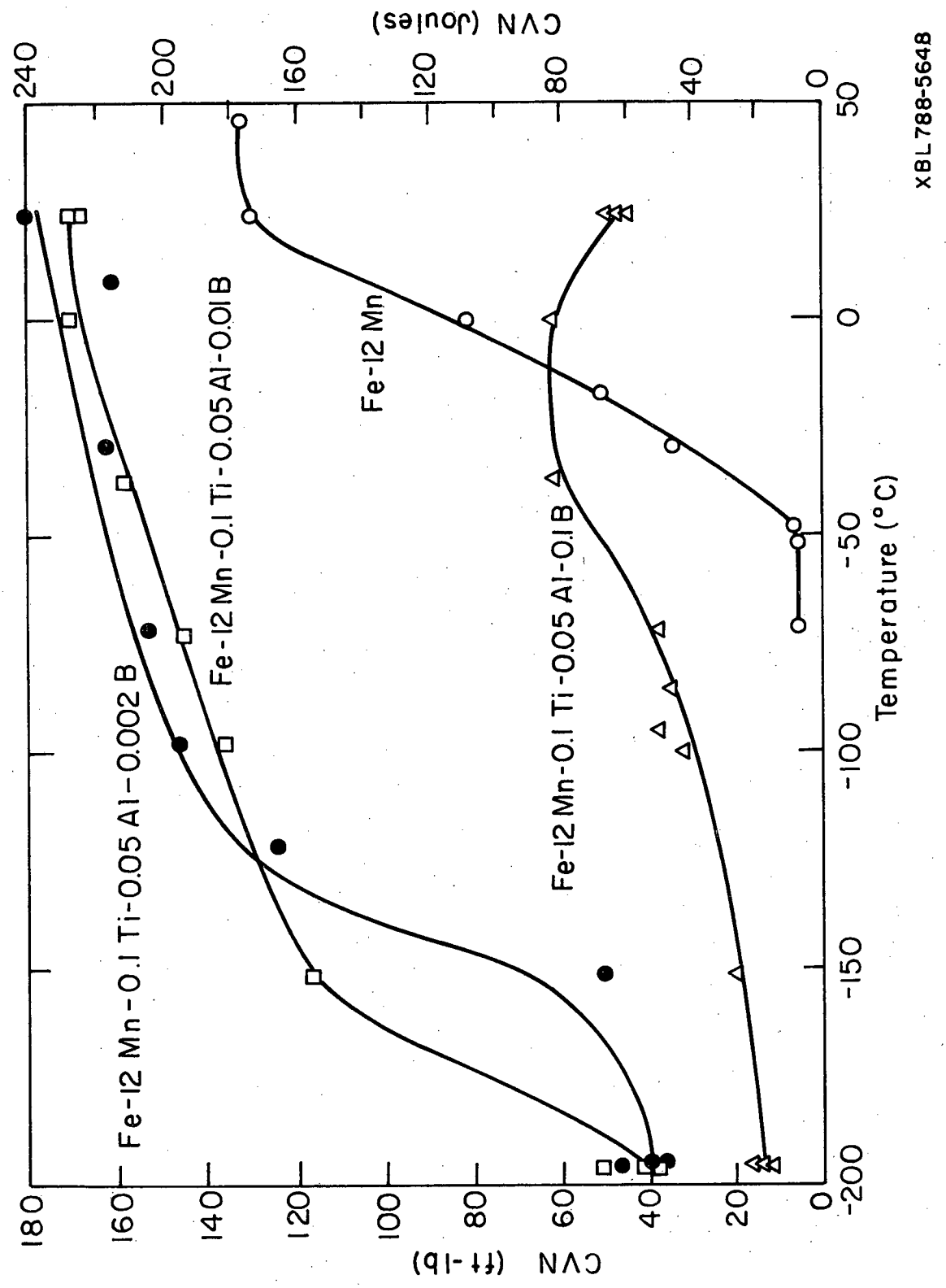
CVN (ft-lb)
CVN (Joules)
Temperature (°C)
Fe-12 Mn-0.1 Ti-0.05 Al-0.002 B
Fe-12 Mn-0.1 Ti-0.05 Al-0.01 B
Fe-12 Mn
Fe-12 Mn-0.1 Ti-0.05 Al-0.1 B
XBL 788-5648

Figure 12

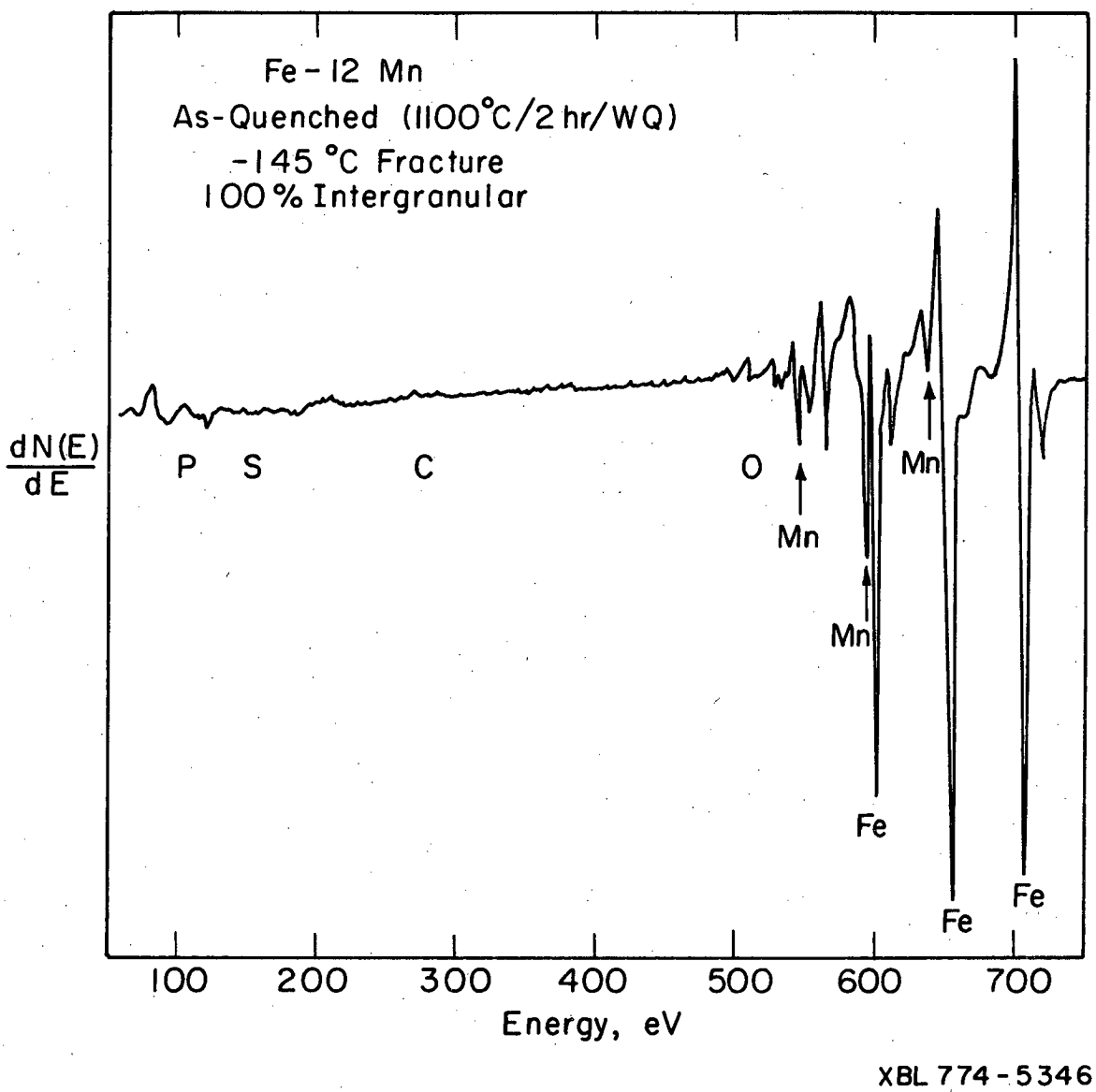
Fe - 12 Mn
As-Quenched (1100°C/2 hr/WQ)
-145 °C Fracture
100 % Intergranular
dN(E)/dE
P
S
C
O
Mn
Mn
Mn
Fe
Fe
Fe
100
200
300
400
500
600
700
Energy, eV
XBL 774-5346

Figure 13

This report was done with support from the Department of Energy. Any conclusions or opinions expressed in this report represent solely those of the author(s) and not necessarily those of The Regents of the University of California, the Lawrence Berkeley Laboratory or the Department of Energy.

Reference to a company or product name does not imply approval or recommendation of the product by the University of California or the U.S. Department of Energy to the exclusion of others that may be suitable.

*TECHNICAL INFORMATION DEPARTMENT*
*LAWRENCE BERKELEY LABORATORY*
*UNIVERSITY OF CALIFORNIA*
*BERKELEY, CALIFORNIA 94720*